

AD-A093 692

WISCONSIN UNIV-MADISON DEPT OF CHEMISTRY  
LUMINESCENT PHOTOELECTROCHEMICAL CELLS. 5. MULTIPLE EMISSION FR-ETC(U)  
DEC 80 B R KARAS, H H STRECKERT, R SCHREINER N00014-78-C-0633

F/G 7/4

UNCLASSIFIED

TR-6

NL

1 of 1  
500/2



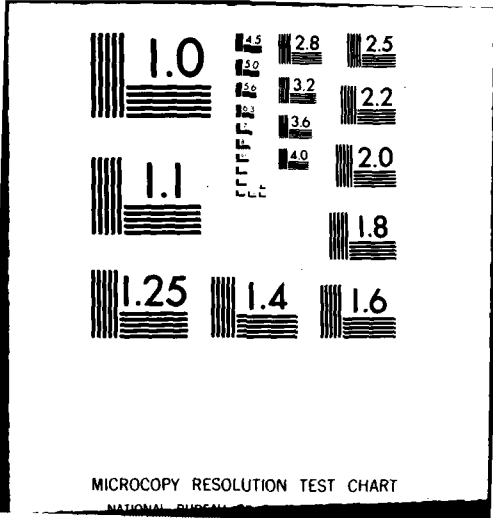
END

DATE

FILED

2 -BI

DTIC



MICROCOPY RESOLUTION TEST CHART

NATIONAL BUREAU OF STANDARDS-1963-A

**LEVEL III**

12

P.S

OFFICE OF NAVAL RESEARCH

Contract No. <sup>15</sup> N00014-78-C-0633

Task No. NR 051-690

9 TECHNICAL REPORT, NO. 6

6  
Luminescent Photoelectrochemical Cells. 5. Multiple Emission from Tellurium-Doped Cadmium Sulfide Photoelectrodes and Implications Regarding Excited-State Communication

14 TR-6

by

10 Bradley R./Karas, Holger H./Streckert, Rodney/Schreiner, and Arthur B./Ellis

226

Prepared for Publication

in the

Journal of the American Chemical Society

Department of Chemistry  
University of Wisconsin  
Madison, Wisconsin 53706

DTIC  
ELECTE  
S  
JAN 13 1981  
E

11 3 December 8, 1980

Reproduction in whole or in part is permitted for any purpose of the United States Government

Approved for Public Release: Distribution Unlimited

\*To whom all correspondence should be addressed.

AD A 093692

FILE COPY

380155

81 1 13 072

JOB

Unclassified

SECURITY CLASSIFICATION OF THIS PAGE (When Data Entered)

REPORT DOCUMENTATION PAGE		READ INSTRUCTIONS BEFORE COMPLETING FORM
1. REPORT NUMBER TECHNICAL REPORT NO. 6	2. GOVT ACCESSION NO. AD-A093692	3. RECIPIENT'S CATALOG NUMBER
4. TITLE (and Subtitle) Luminescent Photoelectrochemical Cells. 5. Multiple Emission from Tellurium-Doped Cadmium Sulfide Photoelectrodes and Implications Regarding Excited-State Communication	5. TYPE OF REPORT & PERIOD COVERED	
7. AUTHOR(s) Bradley R. Karas, Holger H. Streckert, Rodney Schreiner, and Arthur B. Ellis	6. PERFORMING ORG. REPORT NUMBER	
9. PERFORMING ORGANIZATION NAME AND ADDRESS Department of Chemistry, University of Wisconsin, Madison, Wisconsin 53706	8. CONTRACT OR GRANT NUMBER(s) N00014-C-78-0633	
11. CONTROLLING OFFICE NAME AND ADDRESS Office of Naval Research/Chemistry Program Arlington, Virginia 22217	10. PROGRAM ELEMENT, PROJECT, TASK AREA & WORK UNIT NUMBERS NR 051-690	
14. MONITORING AGENCY NAME & ADDRESS (if different from Controlling Office)	12. REPORT DATE December 3, 1980	
	13. NUMBER OF PAGES 19	
16. DISTRIBUTION STATEMENT (of this Report)  Approved for Public Release: Distribution Unlimited	15. SECURITY CLASS. (of this report) Unclassified	
	15a. DECLASSIFICATION/DOWNGRADING SCHEDULE	
17. DISTRIBUTION STATEMENT (of the abstract entered in Block 20, if different from Report)		
18. SUPPLEMENTARY NOTES Prepared for publication in the Journal of the American Chemical Society.		
19. KEY WORDS (Continue on reverse side if necessary and identify by block number) Photoelectrochemistry; luminescence; cadmium sulfide electrodes  <i>λ<sub>max</sub> ≈ 510 nm</i> <i>λ<sub>max</sub> ≈ 600 nm</i>		
20. ABSTRACT (Continue on reverse side if necessary and identify by block number) Samples of single-crystal, n-type, 100 ppm Te-doped CdS (CdS:Te) exhibit two emission bands when excited at several ultraband gap wavelengths. One emission band with λ <sub>max</sub> ≈ 510 nm is near the band gap of CdS:Te (≈ 2.4 eV) and is likely edge emission. Its decay time, measured for samples immersed in sulfide solution (1M OH <sup>-</sup> /1M S <sup>2-</sup> ) between 295 and 333 K, is faster than the pulse from the N <sub>2</sub> -pumped dye laser (≈ 7 nsec) used for 458-nm excitation. The other emissive transition, λ <sub>max</sub> ≈ 600 nm, involves intraband gap states		

DD FORM 1473 JAN 73

EDITION OF 1 NOV 68 IS OBSOLETE  
S/N 0102-LP-014-6601

Unclassified

SECURITY CLASSIFICATION OF THIS PAGE (When Data Entered)

Unclassified

SECURITY CLASSIFICATION OF THIS PAGE (When Data Entered)

*tau sub 1/e*

*less than*

introduced by Te. Intensity-time curves for this band have rise times of 310 nsec and generally exhibit nonexponential decay; values of  $\tau_{1/e}$  are typically  $120 \pm 40$  and  $80 \pm 30$  nsec at 295 and 333 K, respectively. When CdS:Te is used as the photoanode in a photoelectrochemical cell employing sulfide electrolyte, both emission bands are quenched in parallel during passage of photocurrent resulting from 457.9- or 476.5-nm Ar ion laser excitation. Parallel quenching is observed at several temperatures for which the excited-state kinetic schemes are demonstrably different: open-circuit emission spectra reveal that both the absolute and relative intensities of the two emission bands are affected by temperature. With increasing temperature (295-333 K) the absolute intensities of both bands decline; a semilog plot of the ratio of 510- to 600-nm intensity vs.  $T^{-1}$  is linear with a slope of  $\sim 0.2$  eV, corresponding to the energy gap between the two excited states. The existence of excited-state communication is inferred from the effects of temperature and electrode potential on multiple emission. Schemes for communication which are compatible with these results are discussed.

*T to the*

<b>Accession For</b>	
NTIS GRA&I	<input checked="" type="checkbox"/>
DTIC TAB	<input type="checkbox"/>
Unannounced	<input type="checkbox"/>
Justification	
By	
Distribution/	
Availability Codes	
Dist	Avail and/or Special
<b>A</b>	

Unclassified

SECURITY CLASSIFICATION OF THIS PAGE (When Data Entered)

## Introduction

We recently reported that the emissive properties of n-type, tellurium-doped CdS (CdS:Te) electrodes can be used to probe electron-hole ( $e^-h^+$ ) pair recombination processes in photoelectrochemical cells (PECs).<sup>2</sup> In particular, emission intensity was found to be dependent on excitation wavelength and intensity, temperature, and electrode potential in a manner consistent with the photoelectrochemical band bending model.<sup>3</sup> A single emission band of sub-band gap energy was monitored in these studies ( $\lambda_{\text{max}} \sim 600$  nm; the band gap,  $E_{\text{BG}}$ , of CdS:Te at low [Te] is believed<sup>4</sup> to be similar to that of undoped CdS,  $\sim 2.4$  eV<sup>5</sup> for which  $\lambda \sim 520$  nm).

While examining electroluminescence from CdS:Te, we saw, in addition to the 600-nm band, a second emission band of approximately band gap energy; both bands could also be observed in photoluminescence experiments under some conditions.<sup>6</sup> In this paper we utilize the energetic and kinetic features of multiple emission to construct a more detailed picture of the CdS:Te excited-state manifold and decay processes. In particular, by examining the effects of temperature and electrode potential on multiple emission, we demonstrate that excited-state communication may be inferred and characterized from PEC experiments.

## Results and Discussion

The samples of single-crystal, n-type, 100 ppm CdS:Te employed in this study exhibited two emission bands when excited at several ultraband gap wavelengths. Multiple emission was visibly apparent when the samples were excited at 337 nm with an intense,  $\text{H}_2$  laser pulse: surface-localized green emission was evident at the site of irradiation in addition to the global orange emission previously reported.<sup>2a</sup> The discrepancy in spatial distribution likely stems from the considerably greater absorptivity of CdS:Te for green light.

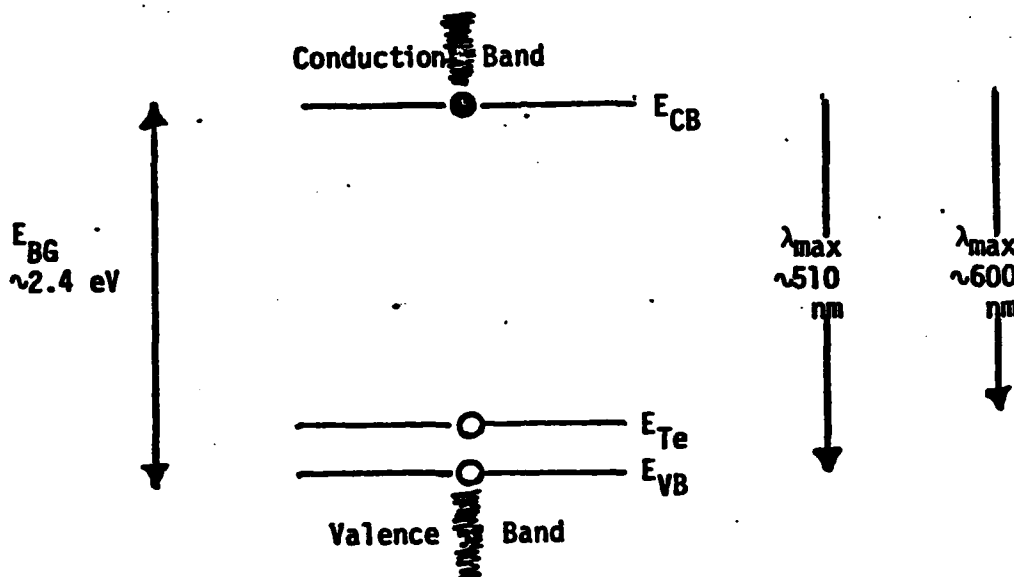
In sections below we discuss the spectral distribution and origin of the two emission bands, their decay times, and the effects of temperature upon emissive properties. The influence of electrode potential on multiple emission is characterized using CdS:Te-based PECs. The final section of the paper is devoted to a description of several excited-state decay schemes which are consistent with our data.

1. Spectral Distribution and Origin of Luminescence

The 295 K, uncorrected, front-surface emission spectrum of single-crystal, n-type, 100 ppm CdS:Te is shown in curve 1 of Figure 1a. Two distinct emission bands - one sharp with  $\lambda_{max} \sim 510$  nm, the other broad with  $\lambda_{max} \sim 600$  nm - are observed for the dry crystal or, as displayed here, out of circuit in transparent sulfide (1M OH<sup>-</sup>/1M S<sup>2-</sup>) electrolyte. The 457.9-nm line of an Ar ion laser is the excitation source.

Both 100 ppm CdS:Te and nominally undoped CdS samples exhibit the 510-nm band whose energy falls near the 2.4 eV band gap of CdS. Given its energy, sharpness, short lifetime (vide infra) and literature precedent,<sup>7</sup> this band is most likely edge emission in both CdS and CdS:Te. Additional support for such an assignment comes from the observed blue-shift of  $\lambda_{max}$  for this band to  $\sim 490$  nm at 77 K. This shift is in reasonable accord with the CdS optical band gap temperature coefficient of  $-5.2 \times 10^{-4}$  eV/K.<sup>8</sup> In contrast, the 600-nm band exhibits a much smaller blue-shift in  $\lambda_{max}$  ( $\leq 10$  nm) in passing from room temperature to 77 K.<sup>2a,9</sup> The 600-nm band has been assigned to a transition involving intraband gap states introduced by the lattice substitution of Te for S; holes trapped in these states, estimated to lie  $\sim 0.2$ eV above the valence band edge, can recombine with electrons in or near the conduction band to yield the observed emission.<sup>4,9</sup> Scheme I incorporates these assignments into a crude energy diagram in which filled

and open circles represent electrons and holes, respectively; the symbols  $E_{CB}$ ,  $E_{VB}$  and  $E_{Te}$  denote energies of the conduction and valence band edges and of the Te states, respectively. In this scheme the energy of an electron increases in the upward direction, while that of a hole increases in the downward direction.



Scheme I

## 2. Decay Times

Besides their different spectral distributions, another feature which distinguishes the two emission bands is their decay times. Excited-state decay times for the two bands were examined in sulfide medium using 458-nm excitation from a  $N_2$ -pumped dye laser. Representative intensity-time curves obtained under these conditions are pictured in Figure 2. The decay profile of the 510-nm band roughly parallels that of the laser pulse, Figure 2a, and indicates that the decay time is  $<10 \text{ nsec}$ ; no significant change in the decay profile is observed between 295 and 333 K. Although our inability to obtain a more precise value for the 510-nm band is disappointing, we note that a decay time in the nanosecond regime is consistent with the presumed strongly allowed nature of this electronic transition.<sup>10</sup>

The intensity-time curves from which the 600-nm decay time is estimated, illustrated in Figure 2b, have rise times of <10 nsec and generally exhibit nonexponential decay; typical  $\tau_{1/e}$  values (measured after a delay of 20 nsec from the maximum intensity of the decay profile) at 295 and 333 K are  $120 \pm 40$  and  $80 \pm 30$  nsec, respectively. Excitation from electron beams,<sup>4b</sup> a  $N_2$  laser,<sup>9</sup> and  $\alpha$  particles<sup>11</sup> have been reported to give 295 K decay times ( $\tau_{1/e}$ ) as disparate as 1000, 300, and 25 nsec, respectively. The discrepancy in our decay times and those in the literature probably reflects the use of different samples and excitation techniques. Our data do accord with results obtained by Perone, Richardson, *et al.* using samples and excitation conditions more akin to those employed here.<sup>12</sup> Their results also indicate that the 295 K decay time of the 600-nm band is somewhat intensity dependent; from measurements of incident energy per pulse at 458 nm, we estimate that peak powers and intensities of  $\sim 2$  kW and  $\sim 100$  kW/cm<sup>2</sup>, respectively, were used in this study.

An important consequence of the inequality in 510- and 600-nm decay times is that it indicates the two excited states are not in thermal equilibrium between 295 and 333 K under the pulse conditions employed.<sup>13</sup> To our knowledge there is no evidence for electron traps at depths comparable to that of the hole trap at  $E_{Te}$ . Consequently, we attribute lack of thermalization to the holes: hole migration between  $E_{Te}$  and  $E_{VB}$  (Scheme I) is not sufficiently rapid relative to  $e^-h^+$  recombination rates to permit the establishment of thermal equilibrium on the time scale of the pulse experiment.

### 3. Temperature Effects

The temperature dependence of the two emission bands is illustrated by the curves labelled "1" in each of Fig. 1a, b, and c, corresponding to the open-circuit emission spectra of CdS:Te in sulfide electrolyte at 295, 312, and 333 K, respectively. Only changes in the intensities and not in the spectral distributions of the individual bands are observed over this temperature range.

Although both bands lose intensity with increasing temperature, the 600-nm band declines more rapidly. Its intensity falls by a factor of  $\sim 4$  over the  $40^\circ$  thermal excursion, in agreement with our earlier results.<sup>2c</sup> A comparatively modest 50% decrease in intensity is observed for the 510-nm band. These changes are reversible upon cooling.

Thermal quenching of the 600-nm band of CdS:Te has been ascribed to the activation energy required to promote Te-bound holes back to the valence band.<sup>4,9,11</sup> At the temperatures employed in this study, repopulation of the upper excited state from the lower excited state would be expected for a  $\sim 0.2$  eV energetic separation. Evidence for thermal repopulation at steady state is provided by Figure 1: a semilog plot of the open-circuit intensity ratio (intensity at 510 nm divided by intensity at 600 nm) vs. reciprocal temperature yields a straight line whose slope is the anticipated activation energy of  $\sim 0.2$  eV.

We had hoped to see back population of the upper excited state reflected in the time-resolved experiments. However, attempts to observe delayed 510-nm emission have thus far been unsuccessful. We ascribe the absence of delayed emission to both the low radiative efficiency of the excited state and the insensitivity of our detection system. Only if the delayed emission intensity had reached a significant fraction ( $\sim 10\%$ ) of the prompt emission intensity would we have detected it.

#### 4. PEC Properties

We turn now to the emissive properties of CdS:Te in the context of a PEC. We previously demonstrated that when a CdS:Te photoanode is excited with ultraband gap radiation in a PEC employing polychalcogenide electrolyte, its 600-nm emission band can be quenched by passing photocurrent;<sup>2</sup> in moving to more positive potentials, increased band bending enhances photocurrent by inhibiting  $e^- - h^+$  pair recombination.<sup>3</sup>

Curves 1-5 of Fig. 1 are the emission spectra observed for the 100 ppm CdS:Te electrode in sulfide electrolyte at increasingly positive bias. The most positive potential of +0.7 V vs. a Ag pseudoreference electrode (PRE) resulted at each temperature in maximum photocurrents of  $\sim 3.1 \text{ mA/cm}^2$  (a photocurrent quantum efficiency of  $\sim 0.8$ ) and minimum emission intensities. The crucial result is that at all three temperatures both emission bands are quenched essentially in parallel by passing photocurrent.

Another presentation of parallel quenching is afforded by Figure 3 which shows the complete current-luminescence-voltage (iLV) curve corresponding to Figure 1a. The top portion of Figure 3 was constructed by arbitrarily scaling up the 510-nm emission intensity to match that at 600 nm at open circuit and then scaling up the 510-nm intensity at the other potentials by this same factor. Within experimental error the two curves are congruent. We also found that 476.5-nm excitation yielded very similar results to those presented here using 457.9-nm light.

##### 5. Mechanistic Implications

Parallel quenching of multiple emission by passing photocurrent implicates the existence of a mechanism for excited-state communication. Such an interpretation is reinforced by the temperature behavior exhibited in Figure 1: the open-circuit curves demonstrate that at three different temperatures three different sets of excited-state rate constants obtain, yet parallel quenching persists. In this section we examine various excited-state kinetic schemes which are compatible with our data. Key mechanistic points to be considered include the nature of excited-state population, the extent to which the excited states interconvert, their relative contributions to photocurrent, and the effects of potential on the various excited-state decay routes.

We shall call the excited states associated with the 510- and 600-nm emission bands A and B, respectively. Although both states could be populated directly with the ultraband gap excitation employed, we believe that only state A is populated in this manner. Indirect population of B is suggested by the relative absorptivities involved. Absorptivities of impurity-based transitions are typically orders of magnitude less than the  $\sim 10^5 \text{ cm}^{-1}$  value observed for band-to-band transitions in CdS and CdS:Te.<sup>4,5,14</sup> We thus favor a scheme wherein A is directly populated and subsequently feeds B. Alternatively, we cannot preclude the existence of a higher-energy excited state, C, which could feed A and B. We have, however, no direct evidence for the existence of state C and will subsequently discuss data which argue against its involvement.

The variable temperature data support the notion that not only is B populated by A, but that interconversion between the states is quite competitive with their other decay processes. Recall that the 510- to 600-nm emission intensity ratio, a measure of the relative populations of A and B, is temperature dependent; a semilog plot of this ratio vs.  $T^{-1}$  is linear with a slope equal to the energy gap between the states of  $\sim 0.2 \text{ eV}$ . If not at thermal equilibrium under steady-state conditions, the states appear to be near it.

Quenching for molecular systems possessing multiple excited states has been analyzed in detail.<sup>13b-d</sup> By analogy to molecular systems, parallel quenching of interconverting A and B states will obtain so long as passage of photocurrent does not upset the interconversion of A and B. Disruption of interconversion requires that a considerable fraction of the photocurrent comes from state B. Since we do not observe a significant departure from parallel quenching, we suspect that state A is the principal contributor to photocurrent, i.e., holes are extracted for photocurrent predominantly from  $E_{VB}$  rather than from  $E_{Te}$  (Scheme I). This conclusion is further supported by the similar photocurrent-voltage properties observed with undoped CdS-based PECs for which state B is absent.<sup>2a</sup>

Other schemes which would accommodate parallel quenching include the exoergic feeding of A and/or B by state C with C the contributor of holes to photocurrent. However, the similarity in iLV properties obtained with 476.5- and 457.9-nm excitation (vide supra) suggests that the simpler A and B model is more appropriate: energetically, 476.5 nm is sufficiently proximate to the onset of the 510-nm emission band to effect direct population of state A. We feel that surface states<sup>15</sup> represent a more likely addition to the excited-state manifold than does state C. Although we know little about their role in this system, surface states can influence both excited-state deactivation and charge-transfer processes; their potential effect on the schemes described should be kept in mind.

Implicit in the discussion of quenching has been the assumption that the ratio of radiative to nonradiative recombination efficiency for each of states A and B is unaffected by electrode potential. Relationships observed between emissive and photocurrent quantum efficiencies suggest this to be the case with the particular ratio dependent at least on temperature and excitation wavelength.<sup>2c,16</sup> However, Figure 3 demonstrates that potential can influence this ratio: in passing to the most positive potentials, the emission intensity continues to decline while the photocurrent is essentially invariant. Similar effects were observed for n-type, ZnO-based PECs and ascribed to a deficiency in the electron concentration needed for recombination near the surface, a consequence of the large electric field present.<sup>17</sup> In the case of multiple emission, the effect may not be the same for each excited state. For example, we have occasionally seen deviations from parallel quenching at the most positive potentials employed. These results indicate that electrode potential can, in some cases, alter excited-state processes beyond simply serving to divert a fraction of the excited-state population to photocurrent.

The various schemes outlined above are not to be considered exhaustive, but rather as representing what we regard as likely possibilities. In our estimation the most reasonable scheme compatible with our present data consists of direct

population of A, interconversion of A and B, and generation of photocurrent principally via state A. Discrimination among this mechanism and several of the alternatives offered may be possible by examining systems with different trap depths and by selective population of the trap-based excited state. Such studies are in progress.

### Experimental Section

**Materials.** Plates of vapor-grown, single-crystal undoped CdS and 100 ppm CdS:Te were obtained from Cleveland Crystals, Inc., Cleveland, Ohio; Te concentration is an estimate based on starting quantities. The 10x10x1 mm samples had resistivities of  $\sim 2$  ohm-cm (4 point probe method) and were oriented with their 10x10 mm face perpendicular to the  $c$ -axis. Samples were cut into irregularly-shaped pieces  $\sim 0.15$  cm<sup>2</sup> x 1 mm, etched with 1:10 (v/v) Br<sub>2</sub>/MeOH for  $\sim 15$  s and subsequently transferred to a beaker of MeOH which was placed in an ultrasonic cleaner to remove residual Br. Etched samples were used either unmounted for decay time studies or mounted as electrodes in a manner previously described.<sup>2a</sup> The preparation of sulfide electrolyte has also been described.<sup>2a</sup>

**Optical Measurements.** Uncorrected emission spectra were obtained with an Aminco-Bowman spectrophotofluorometer (200-800 nm; bandwidth  $\sim 5$  nm) equipped with a Hamamatsu R446S PMT for extended red response. Spectra were displayed on a HP 7004A x-y recorder. Sample excitation was achieved by passing the 2-3 mm diameter beam of a Coherent Radiation CR-12 Ar ion laser through a Melles Griot 03-FCG055 long-pass filter (cutoff  $\sim 380$  nm), 10X expanding the beam, and translating it upward via a periscope into a hole in the side of the spectrometer compartment. The beam was masked at this point in PEC experiments to fill the electrode surface. Residual exciting light was filtered from the emitted light by placing an aqueous 1M OH<sup>-</sup>/1M S<sup>2-</sup>/0.2M S polysulfide solution in front of the PMT. Laser intensity was measured with a Tektronix J16 radiometer equipped with a J6502 probe head (flat response  $\pm 7\%$ , 450-950 nm). For continuous monitoring of intensity, a quartz

disk was used to split part of the beam into a Scientech 362 power meter whose output was recorded on a Heath Model EU-205-11 strip chart recorder. Emission spectra at 77 K were obtained by placing CdS:Te samples in a 21 cm x 7 mm o.d. tube inserted into a Dewar designed to fit into the emission spectrometer chamber. The sample was cooled with liquid N<sub>2</sub> and the spectrum recorded. Without disturbing the geometry, the liquid N<sub>2</sub> was allowed to evaporate and the spectrum recorded again after the sample had warmed back to 295 K. Condensation of water on the Dewar was prevented by continuously purging the sample compartment with N<sub>2</sub>.

**Decay Time Measurements.** Samples of CdS:Te were excited with the output of an NRG DL 0.03 dye laser ( $\sim 7$  nsec FWHM) which was pumped by an NRG - 0.7-5-200 pulsed N<sub>2</sub> laser (0.7 MW peak power). The detection system consisted of (in series) a Bausch & Lomb Model 33-86-07 monochromator (bandwidth  $\sim 10$  nm), a ferricyanide filter solution (0.6 M K<sub>3</sub>Fe(CN)<sub>6</sub>/0.6 M HCl; 1.0 cm pathlength cell) to absorb the exciting light, and a Hamamatsu R928 PMT whose base permitted the output to be fed directly into a Tektronix Model 466 storage oscilloscope. Decay curves were obtained by operating the oscilloscope in variable persistence mode which averaged several hundred pulses. Generally, the laser was run at 20 or 30 pulses per second. A 7.0 cm x 2.5 cm o.d. Pyrex vessel was used to hold sulfide electrolyte into which the CdS:Te samples, held by Teflon-coated tweezers, were suspended. The sulfide electrolyte was continuously purged by N<sub>2</sub> via a distilled water reservoir (to maintain solution volume) during the measurements. Samples were positioned at  $\sim 45^\circ$  to both the  $\sim 0.02$  cm<sup>2</sup> laser beam and the monochromator entrance slit, but the angle was offset slightly to minimize collection of the reflected laser light by the detection optics. Temperature was varied by resistively heating a nichrome wire which surrounded the Pyrex vessel; a calibrated thermometer was used to measure the temperature of the solution. Laser intensity was estimated by accumulating the energy from

## References and Notes

1. Parts 3 and 4 of this series are references 2c and 6, respectively.
2. (a) Karas, B.R.; Ellis, A.B. J. Amer. Chem. Soc. 1980, 102, 968;  
(b) Ellis, A.B.; Karas, B.R. Adv. Chem. Ser. 1980, 184, 185;  
(c) Karas, B.R.; Morano, D.J.; Billich, D.K.; Ellis, A.B. J. Electrochem. Soc. 1980, 127, 1144.
3. Gerischer, H. J. Electroanal. Chem. 1975, 58, 263.
4. (a) Aten, A.C.; Haanstra, J.H.; deVries, H. Philips Res. Rep. 1965, 20, 395;  
(b) Cuthbert, J.D.; Thomas, D.G. J. Appl. Phys. 1968, 39, 1573;  
(c) Moulton, P.F. Ph.D. Dissertation, Massachusetts Institute of Technology, 1975.
5. Dutton, D. Phys. Rev. 1958, 112, 785.
6. Streckert, H.H.; Karas, B.R.; Morano, D.J.; Ellis, A.B. J. Phys. Chem., in press.
7. (a) Kulp, B.A.; Detweiler, R.M.; Anders, W.A. Phys. Rev. 1963, 131, 2036 and references therein; (b) Halsted, R.E. in "Physics and Chemistry of II-VI Compounds", Aven, M.; Prener, J.S., Eds. North Holland Publishing Co., Amsterdam, 1967, Ch. 8.
8. Bube, R.H. Phys. Rev., 1954, 98, 431.
9. Roessler, D.M. J. Appl. Phys. 1970, 41, 4589.
10. Pankove, J.I. "Optical Processes in Semiconductors", Prentice-Hall, Inc. New Jersey, 1971. Ch. 6.
11. Bateman, J.E.; Ozsan, F.E.; Woods, J.; Cutter, J.R. J. Phys. D. Appl. Phys. 1974, 7, 1316.
12. S. P. Perone and J.H. Richardson, private communication (submitted for publication).

~400 pulses with the Scientech power meter and correcting for background radiation over the 20 s data collection period.

**PEC Experiments.** A CdS:Te working electrode, a Pt counterelectrode, a Ag pseudoreference electrode (PRE), a magnetic stir bar, and sulfide electrolyte were all placed in the Pyrex vessel which was positioned in the sample compartment of the emission spectrometer. The CdS:Te electrode was oriented at ~45° to both the exciting Ar ion laser beam and the emission detection optics so that principally front-surface emission was detected. A motorized magnet placed beneath the sample chamber was used to stir the electrolyte which was purged by N<sub>2</sub> and heated as described above. Electrode potential was controlled by a PAR 173 potentiostat/galvanostat with current (PAR 176 I/E converter) displayed on a Varian 9176 strip-chart recorder. Current-luminescence-voltage (iLV) curves were taken point-by-point at 295, 312, 333 and 295 K again to demonstrate reproducibility; emission spectra were recorded at each potential as described under Optical Measurements (vide supra). Incident light intensity was determined by reassembling the PEC outside of the emission spectrometer; the intensity which produced the same i-V properties was measured with the Tektronix radiometer. Photocurrent in these experiments appeared to be excitation-rate limited, since it varied linearly with light intensity and was not influenced by stirring rate.

**Acknowledgment** We are grateful to the Office of Naval Research for support of this work. Dr. David Lang of Bell Laboratories and Professor Peter Wagner of Michigan State University are acknowledged for helpful discussions.

13. (a) DiBartolo, B. "Optical Interactions in Solids", John Wiley & Sons, Inc. New York, 1968, Ch. 18.3; (b) Wagner, P.J. in "Creation and Detection of the Excited State", Lamola, A.A. Ed., Vol. I, Part A., Marcel Dekker, New York, 1971, Ch. 4.; (c) Shetlar, M.D. Mol. Photochem. 1974, 6, 143, 167, 191; (d) Wagner, P.J. J. Photochem. 1979, 10, 387.
14. Reference 10, Ch. 3.
15. Bard, A.J.; Bocarsly, A.B.; Fan, F.F.; Walton, E.G.; Wrighton, M.S. J. Am. Chem. Soc. 1980, 102, 3671 and references therein.
16. Ellis, A.B.; Karas, B.R.; Streckert, H.H. Faraday Discuss. Chem. Soc. in press.
17. Petermann, G.; Tributsch, H.; Bogomolni, R. J. Chem. Phys. 1972, 57, 1026.

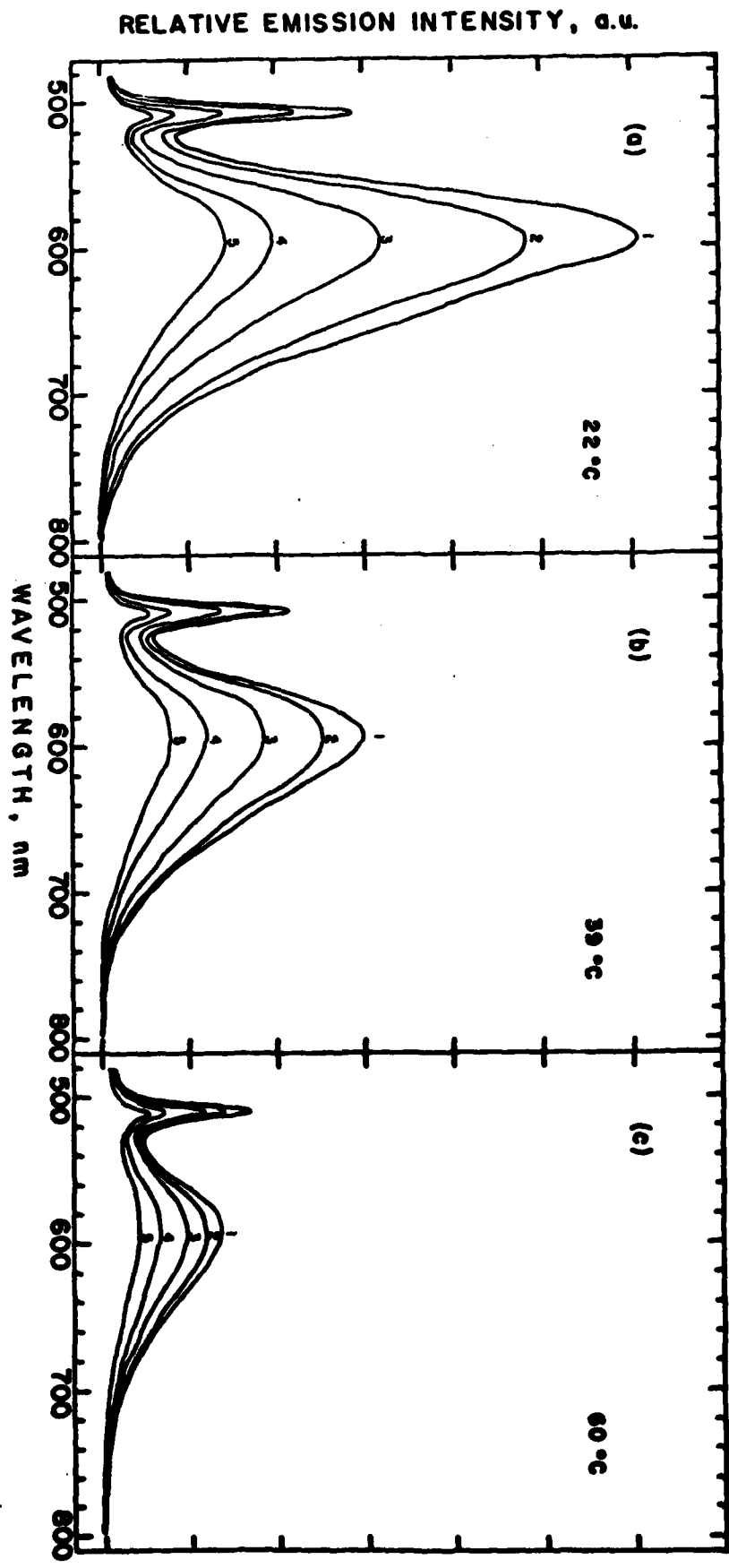
### Figure Captions

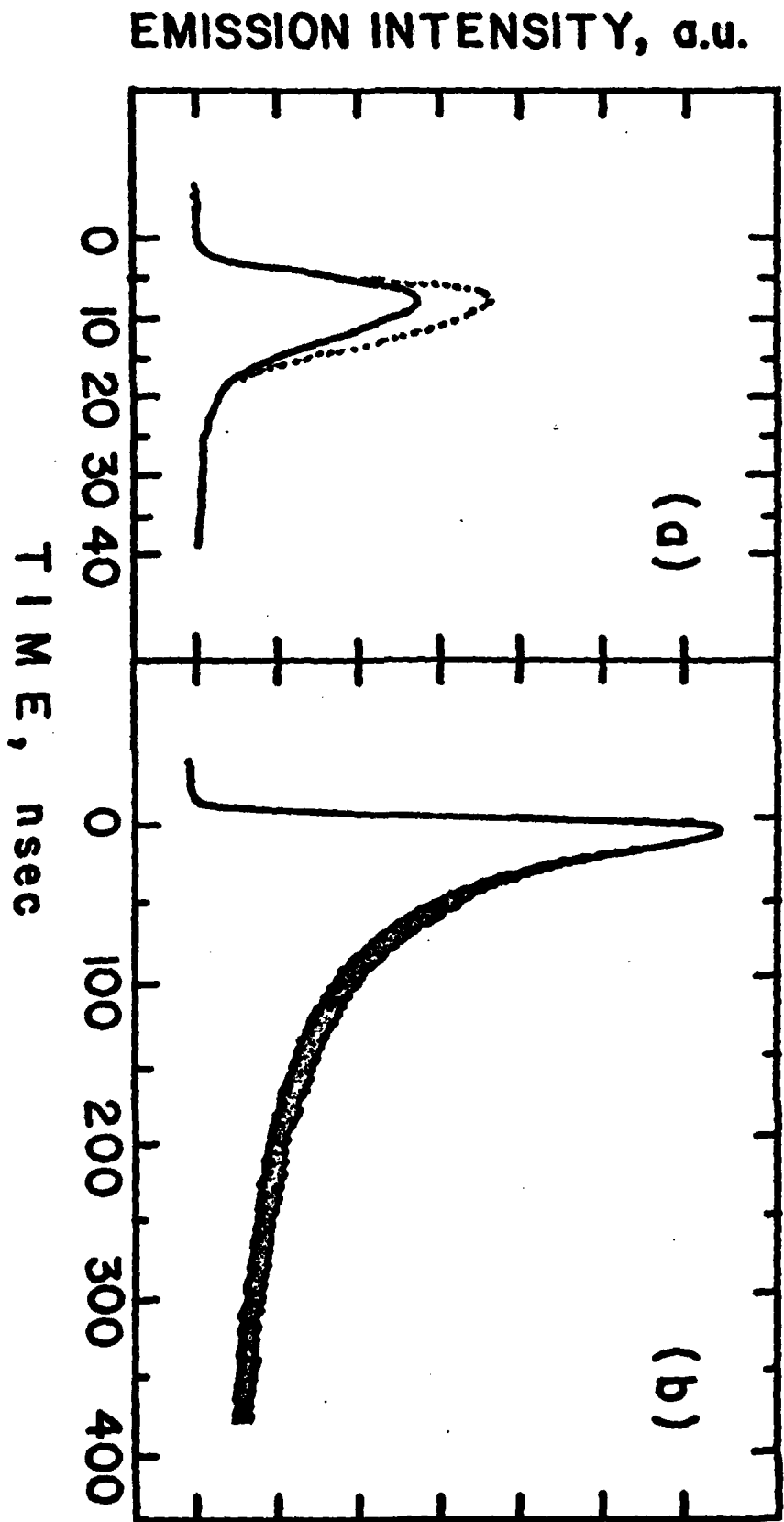
Figure 1. Uncorrected emission spectra of a 100 ppm CdS:Te electrode as a function of potential and temperature in sulfide ( $1M OH^-/1M S^{2-}$ ) electrolyte. Frames a, b, and c are data taken at 295, 312 and 333 K, respectively. Curves 1, 2, 3, 4 and 5 in each frame correspond to open circuit, -0.5, -0.3, +0.15 and +0.7 V vs. Ag (PRE), respectively. Pt foil (1x3 cm) served as the counter-electrode in the  $N_2$ -purged PEC. Because PEC geometry and incident intensity ( $\sim 1.7$  mW of 457.9-nm excitation incident on the  $0.16$  cm<sup>2</sup> CdS:Te exposed surface area) were unchanged throughout these experiments, the emissive intensities pictured are directly comparable.

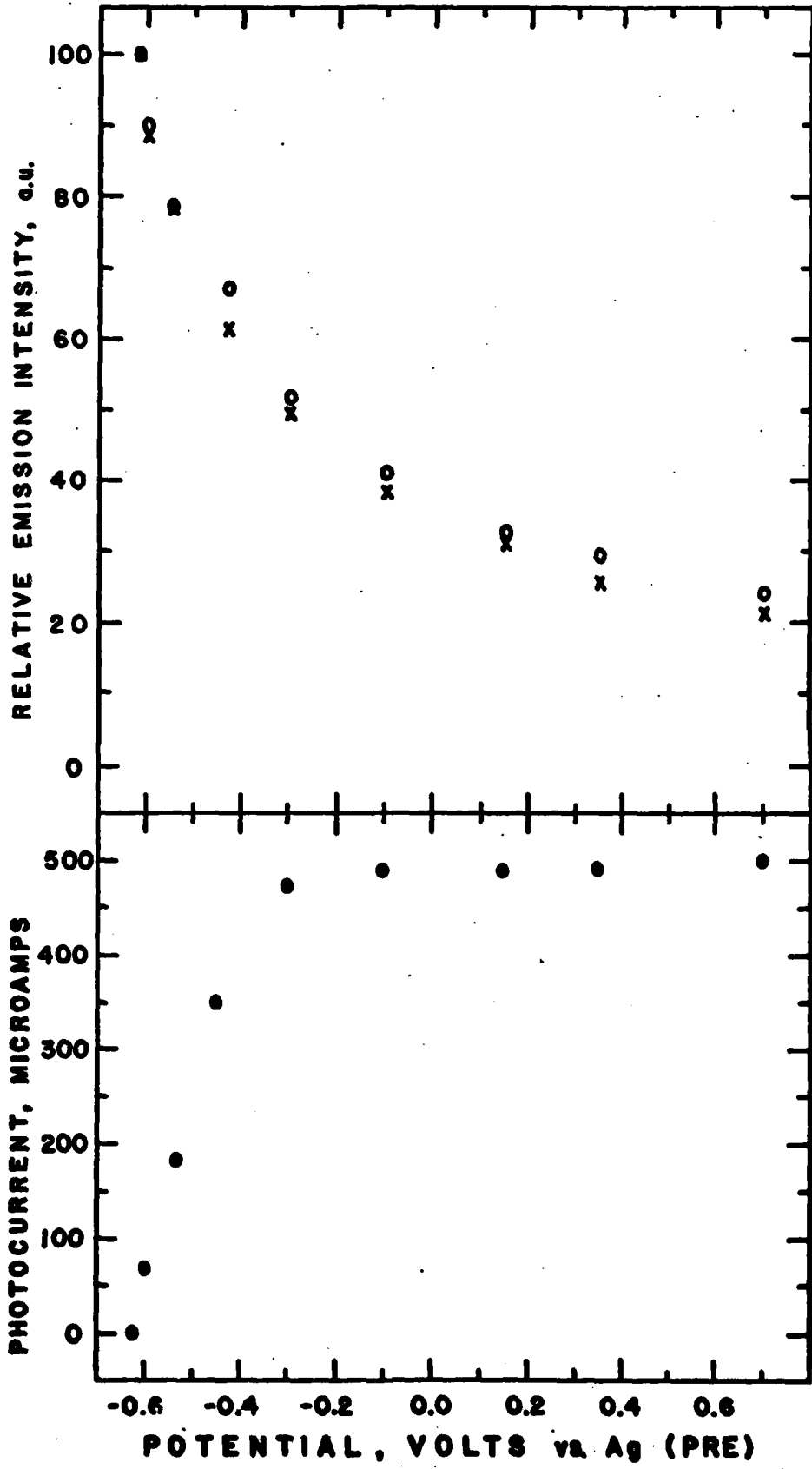
Figure 2. Representative intensity-time curves of the 510-nm emission band ((a), solid line) and the 600-nm emission band (b). These curves were obtained at 295 K using a  $\sim 0.16$  cm<sup>2</sup>, 100 ppm, single-crystal CdS:Te sample suspended in sulfide electrolyte and excited at 458 nm with a  $N_2$ -pumped dye laser. The intensity-time profile of the excitation source is displayed as the dotted curve in (a).

Incident peak power delivered in a typical pulse is estimated to be  $\sim 2$  kW over an area of  $\sim 0.02$  cm<sup>2</sup>. Intensities of the three curves are not directly comparable, since they were recorded at different sensitivities.

Figure 3. Photocurrent (bottom frame) and emission intensity (top frame), monitored at 510 nm (X) and 600 nm (O), vs. electrode potential for the 295 K experiment of Figure 1. The open-circuit emission intensity at 600 nm has been arbitrarily set at 100 with the 510-nm emission intensity scaled up to match this value. The 510-nm intensity at other potentials was then scaled up by this same factor to obtain the data pictured.







TECHNICAL REPORT DISTRIBUTION LIST, GEN

	<u>No. Copies</u>		<u>No. Copies</u>
Dr. Jerry J. Smith			
Office of Naval Research Attn: Code 472 800 North Quincy Street Arlington, Virginia 22217	2	U.S. Army Research Office Attn: CRD-AA-IP P.O. Box 1211 Research Triangle Park, N.C. 27709	1
ONR Branch Office Attn: Dr. George Sandoz 536 S. Clark Street Chicago, Illinois 60605	1	Naval Ocean Systems Center Attn: Mr. Joe McCartney San Diego, California 92152	1
ONR Western Regional Office 1030 East Green Street Pasadena, California 91106	1	Naval Weapons Center Attn: Dr. A. B. Amster, Chemistry Division China Lake, California 93555	1
ONR Eastern/Central Regional Office Attn: Dr. L. H. Peebles Building 114, Section D 666 Summer Street Boston, Massachusetts 02210	1	Naval Civil Engineering Laboratory Attn: Dr. R. W. Drisko Port Hueneme, California 93401	1
Director, Naval Research Laboratory Attn: Code 6100 Washington, D.C. 20390	1	Department of Physics & Chemistry Naval Postgraduate School Monterey, California 93940	1
The Assistant Secretary of the Navy (RE&S) Department of the Navy Room 4E736, Pentagon Washington, D.C. 20350	1	Dr. A. L. Slafkosky Scientific Advisor Commandant of the Marine Corps (Code RD-1) Washington, D.C. 20380	1
Commander, Naval Air Systems Command Attn: Code 310C (H. Rosenwasser) Department of the Navy Washington, D.C. 20360	1	Office of Naval Research Attn: Dr. Richard S. Miller 800 N. Quincy Street Arlington, Virginia 22217	1
Defense Technical Information Center Building 5, Cameron Station Alexandria, Virginia 22314	12	Naval Ship Research and Development Center Attn: Dr. G. Bosmajian, Applied Chemistry Division Annapolis, Maryland 21401	1
Dr. Fred Saalfeld Chemistry Division, Code 6100 Naval Research Laboratory Washington, D.C. 20375	1	Naval Ocean Systems Center Attn: Dr. S. Yamamoto, Marine Sciences Division San Diego, California 91232	1
		Mr. John Boyle Materials Branch Naval Ship Engineering Center Philadelphia, Pennsylvania 19112	1

TECHNICAL REPORT DISTRIBUTION LIST, GEN

	<u>No.</u>
	<u>Copies</u>
Dr. Rudolph J. Marcus Office of Naval Research Scientific Liaison Group American Embassy APO San Francisco 96503	1
Mr. James Kelley DTNSRDC Code 2803 Annapolis, Maryland 21402	1

TECHNICAL REPORT DISTRIBUTION LIST, 359

	<u>No. Copies</u>		<u>No. Copies</u>
Dr. Paul Delahay Department of Chemistry New York University New York, New York 10003	1	Dr. P. J. Hendra Department of Chemistry University of Southampton Southampton SO9 5NH United Kingdom	1
Dr. E. Yeager Department of Chemistry Case Western Reserve University Cleveland, Ohio 41106	1	Dr. Sam Perone Department of Chemistry Purdue University West Lafayette, Indiana 47907	1
Dr. D. N. Bennion Department of Chemical Engineering Brigham Young University Provo, Utah 84602	1	Dr. Royce W. Murray Department of Chemistry University of North Carolina Chapel Hill, North Carolina 27514	1
Dr. R. A. Marcus Department of Chemistry California Institute of Technology Pasadena, California 91125	1	Naval Ocean Systems Center Attn: Technical Library San Diego, California 92152	1
Dr. J. J. Auburn Bell Laboratories Murray Hill, New Jersey 07974	1	Dr. C. E. Mueller The Electrochemistry Branch Materials Division, Research & Technology Department Naval Surface Weapons Center White Oak Laboratory Silver Spring, Maryland 20910	1
Dr. Adam Heller Bell Laboratories Murray Hill, New Jersey 07974	1	Dr. G. Goodman Globe-Union Incorporated 5757 North Green Bay Avenue Milwaukee, Wisconsin 53201	1
Dr. T. Katan Lockheed Missiles & Space Co, Inc. P.O. Box 504 Sunnyvale, California 94088	1	Dr. J. Boechler Electrochimica Corporation Attention: Technical Library 2485 Charleston Road Mountain View, California 94040	1
Dr. Joseph Singer, Code 302-1 NASA-Lewis 21000 Brookpark Road Cleveland, Ohio 44135	1	Dr. P. P. Schmidt Department of Chemistry Oakland University Rochester, Michigan 48063	1
Dr. B. Brunner EIC Incorporated 55 Chapel Street Newton, Massachusetts 02158	1	Dr. N. Richtol Chemistry Department Rensselaer Polytechnic Institute Troy, New York 12181	1
Library P. R. Mallory and Company, Inc. Northwest Industrial Park Burlington, Massachusetts 01803	1		

TECHNICAL REPORT DISTRIBUTION LIST, 359

	<u>No.</u> <u>Copies</u>		<u>No.</u> <u>Copies</u>
<del>Dr. A. B. Ellis</del> <del>Chemistry Department</del> <del>University of Wisconsin</del> <del>Madison, Wisconsin 53706</del>	<del>1</del>	Dr. R. P. Van Duyne Department of Chemistry Northwestern University Evanston, Illinois 60201	1
Dr. M. Wrighton Chemistry Department Massachusetts Institute of Technology Cambridge, Massachusetts 02139	1	Dr. B. Stanley Pons Department of Chemistry University of Alberta Edmonton, Alberta CANADA T6G 2G2	1
Larry E. Plew Naval Weapons Support Center, Code 30736, Building 2906 Crane, Indiana 47522	1	Dr. Michael J. Weaver Department of Chemistry Michigan State University East Lansing, Michigan 48824	1
S. Rubv DOE (STOR) 600 E Street Washington, D.C. 20545	1	Dr. R. David Rauh EIC Corporation 55 Chapel Street Newton, Massachusetts 02158	1
Dr. Aaron Wold Brown University Department of Chemistry Providence, Rhode Island 02192	1	Dr. J. David Margerum Research Laboratories Division Hughes Aircraft Company 3011 Malibu Canyon Road Malibu, California 90265	1
Dr. R. C. Chudacek McGraw-Edison Company Edison Battery Division Post Office Box 28 Bloomfield, New Jersey 07003	1	Dr. Martin Fleischmann Department of Chemistry University of Southampton Southampton 509 5NH England	1
Dr. A. J. Bard University of Texas Department of Chemistry Austin, Texas 78712	1	Dr. Janet Osteryoung Department of Chemistry State University of New York at Buffalo Buffalo, New York 14214	1
Dr. M. M. Nicholson Electronics Research Center Rockwell International 3370 Miraloma Avenue Anaheim, California	1	Dr. R. A. Osteryoung Department of Chemistry State University of New York at Buffalo Buffalo, New York 14214	1
Dr. Donald W. Ernst Naval Surface Weapons Center Code R-33 White Oak Laboratory Silver Spring, Maryland 20910	1	Mr. James R. Moden Naval Underwater Systems Center Code 3632 Newport, Rhode Island 02840	1

TECHNICAL REPORT DISTRIBUTION LIST, 359

	<u>No. Copies</u>		<u>No. Copies</u>
Dr. R. Nowak Naval Research Laboratory Code 6130 Washington, D.C. 20375	1	Dr. John Kincaid Department of the Navy Strategic Systems Project Office Room 901 Washington, DC 20376	1
Dr. John F. Houlihan Shenango Valley Campus Pennsylvania State University Sharon, Pennsylvania 16146	1	M. L. Robertson Manager, Electrochemical Power Sonices Division Naval Weapons Support Center Crane, Indiana 47522	1
Dr. M. G. Sceats Department of Chemistry University of Rochester Rochester, New York 14627	1	Dr. Elton Cairns Energy & Environment Division Lawrence Berkeley Laboratory University of California Berkeley, California 94720	1
Dr. D. F. Shriver Department of Chemistry Northwestern University Evanston, Illinois 60201	1	Dr. Bernard Spielvogel U.S. Army Research Office P.O. Box 12211 Research Triangle Park, NC 27709	1
Dr. D. H. Whitmore Department of Materials Science Northwestern University Evanston, Illinois 60201	1	Dr. Denton Elliott Air Force Office of Scientific Research Bldg. 104 Bolling AFB Washington, DC 20332	1
Dr. Alan Bewick Department of Chemistry The University Southampton, SO9 5NH England	1		
Dr. A. Himy NAVSEA-5433 NC #4 2541 Jefferson Davis Highway Arlington, Virginia 20362	1		

TECHNICAL REPORT DISTRIBUTION LIST, OS1C

	<u>No.</u> <u>Copies</u>		<u>No.</u> <u>Copies</u>
Dr. M. B. Denton Department of Chemistry University of Arizona Tucson, Arizona 85721	1	Dr. John Duffin United States Naval Postgraduate School Monterey, California 93940	1
Dr. R. A. Osteryoung Department of Chemistry State University of New York at Buffalo Buffalo, New York 14214	1	Dr. G. M. Hieftje Department of Chemistry Indiana University Bloomington, Indiana 47401	1
Dr. B. R. Kowalski Department of Chemistry University of Washington Seattle, Washington 98105	1	Dr. Victor L. Rehn Naval Weapons Center Code 3813 China Lake, California 93555	1
Dr. S. P. Perone Department of Chemistry Purdue University Lafayette, Indiana 47907	1	Dr. Christie G. Enke Michigan State University Department of Chemistry East Lansing, Michigan 48824	1
Dr. D. L. Venezky Naval Research Laboratory Code 6130 Washington, D.C. 20375	1	Dr. Kent Eisentraut, MBT Air Force Materials Laboratory Wright-Patterson AFB, Ohio 45433	1
Dr. H. Freiser Department of Chemistry University of Arizona Tucson, Arizona 85721		Walter G. Cox, Code 3632 Naval Underwater Systems Center Building 148 Newport, Rhode Island 02840	1
Dr. Fred Saalfeld Naval Research Laboratory Code 6110 Washington, D.C. 20375	1	Professor Isiah M. Warner Texas A&M University Department of Chemistry College Station, Texas 77840	1
Dr. H. Chernoff Department of Mathematics Massachusetts Institute of Technology Cambridge, Massachusetts 02139	1	Professor George H. Morrison Cornell University Department of Chemistry Ithaca, New York 14853	1
Dr. K. Wilson Department of Chemistry University of California, San Diego La Jolla, California	1		
Dr. A. Zirino Naval Undersea Center San Diego, California 92132	1		